Inorg. Chem. **2008**, *47*, 999–1006

Synthesis and Molecular and Electronic Structure of an Unusual Paramagnetic Borohydride Complex $Mo(NAr)_2(PMe_3)_2(\eta^2\text{-}BH_4)$†

Andrey Y. Khalimon,[‡] Jason P. Holland,[§] Radoslaw M. Kowalczyk,[||] Eric J. L. McInnes,[||] Jennifer C. Green,*[,§] Philip Mountford,*[,§] and Georgii I. Nikonov*[,‡]

Chemistry Department, Brock University, Glenridge Ave. 500, St Catharines, ON L2S3A1, Canada, Inorganic Chemistry Laboratory, University of Oxford, South Parks Road, Oxford OX1 3QR, U.K., and EPSRC c. w. EPR Service Centre, School of Chemistry, The University of Manchester, Oxford Road, Manchester M13 9PL, U.K.

Received September 15, 2007

Reaction of $Mo(NAr)_2Cl_2(DME)$ (Ar = 2,6-$C_6H_3{}^iPr_2$, DME = 1,2-dimethoxyethane) with $NaBH_4$ and PMe_3 in THF formed the paramagnetic Mo(V) d^1 borohydride complex $Mo(NAr)_2(PMe_3)_2(\eta^2\text{-}BH_4)$ (**1**). Compound **1**, which was characterized by EPR spectroscopy and X-ray diffraction analysis, provides a rare example both of a paramagnetic bis(imido) group 6 compound and a structurally characterized molybdenum borohydride complex. Density functional theory calculations were used to determine the electronic structure and bonding parameters of **1** and showed that it is best viewed as a 19 valence electron compound (having a primarily metal-based SOMO) in which the BH_4^- ligand behaves as a σ-only, 2-electron donor.

Introduction

Transition metal hydrides are ubiquitous in coordination and organometallic chemistry and usually conform to the effective electron number rule, i.e., exhibit either an 18 or 16 (for d^8 complexes) valence electron count.[1] Although complexes with an odd valence shell have become quite common, odd-electron hydrides (e.g., the 17 and 19 valence electron species $Cp_2Ti(\eta^2\text{-}BH_4)$ and $Ni(Triphos)(\eta^2\text{-}BH_4)$, respectively) are relatively rare.[2−4] Steric protection can stabilize electron-deficient centers, as is the case in Poli's 15 valence electron complex $(\eta\text{-}C_5H_2Bu^t{}_3)Mo(H)(PMe_3)_2$,[5] but "electron rich" 19e and 20e configurations usually only occur if there are strong π-accepting ligands, such as CO, NO, and PF_3, which can delocalize the "excess" electron density from the metal.[1]

This research originally stemmed from our interest in studying hydride derivatives in metallocene-like ligand platforms.[6] N-based ligands isolobal with Cp^-, such as R_3PN^-, RN^{2-}, and cyclic triamines, have been recently successfully applied for systematic design of post-metallocene ligand environments, primarily for the application in catalytic olefin polymerization,[7] but relatively little is known about their hydride derivatives.[8] Because the trihydrides [Cp_2-

* To whom correspondence should be addressed. E-mail: philip.mountford@chemistry.oxford.ac.uk (P.M.), gnikonov@brocku.ca (G.I.N.).

† Dedicated to Professor Martyn Poliakoff on the occasion of his 60th birthday.

‡ Brock University.

§ University of Oxford.

|| The University of Manchester.

(1) (a) Crabtree, R. H. *The Organometallic Chemistry of the Transition Metals*, 4th ed.; Wiley: New York, 2005. (b) Crabtree, R. H. Hydrogen and Hydrides as Ligands. In *Comprehensive Inorganic Chemistry*; Wilkinson, G., Ed.; Pergamon: London, Chapter 19.

(2) (a) Poli, R. In *Recent Advances in Hydride Chemistry*; Poli, R., Peruzzini, M., Eds.; Elsevier: Amsterdam, 2001; Chapter 6. (b) Pleune, B.; Morales, D.; Meunier-Prest, R.; Richard, P.; Collange, E.; Fettinger, J. C.; Poli, R. *J. Am. Chem. Soc.* **1999**, *121*, 2209. (c) Fryzuk, M. D.; Johnson, S. A.; Rettig, S. J. *Organometallics* **2000**, *19*, 3931. (d) Jewson, J. D.; Liable-Sands, L. M.; Yap, G. P. A.; Rheingold, A. L.; Theopold, K. H. *Organometallics* **1999**, *18*, 300. (e) Kersten, J. L.; Rheingold, A. L.; Theopold, K. H.; Casey, C. P.; Widenhoefer, R. A.; Hop, C. E. C. *Angew. Chem., Int. Ed.* **1992**, *31*, 1341. (f) Hessen, B.; van Bolhuis, F.; Teuben, J. H. *J. Am. Chem. Soc.* **1988**, *110*, 295. (g) Raynor, J. B.; Sattelberger, A. P.; Luetkens, M. L. *Inorg. Chim. Acta* **1986**, *113*, 51. (h) Bianchini, C.; Meali, C.; Sabat, M. *Chem. Commun.* **1986**, 777. (j) Luetkens, M. L.; Elcesser, W. L.; Huffman, J. C.; Sattelberger, A. P. *Chem. Commun.* **1983**, 1072. (k) Elson, I. H.; Kochi, J. K.; Klabunde, U.; Manzer, L. E.; Parshall, G. W.; Tebbe, F. N. *J. Am. Chem. Soc.* **1974**, *96*, 7374.

(3) Marks, T. J.; Kolb, J. R. *Chem. Rev.* **1977**, *77*, 263.

(4) Examples from borohydride chemistry: (a) Kandiah, M.; McGrady, G. S.; Decken, A.; Sirsch, P. *Inorg. Chem.* **2005**, *44*, 8650. (b) Jensen, J. A.; Girolami, G. S. *Inorg. Chem.* **1989**, *28*, 2107. (c) Jensen, J. A.; Wilson, S. R.; Girolami, G. S. *J. Am. Chem. Soc.* **1988**, *110*, 4977. (d) Jensen, J. A.; Girolami, G. S. *J. Am. Chem. Soc.* **1988**, *110*, 4450. (e) Holan, D. G.; Hueghes, A. N.; Hui, B. C.; Kan, C. T. *Can. J. Chem.* **1978**, *56*, 814. (f) Holan, D. G.; Hueghes, A. N.; Hui, B. C.; Write, K. *Can. J. Chem.* **1974**, *52*, 2990. (g) Melmed, K. M.; Coucouvanis, D.; Lippard, S. J. *Inorg. Chem.* **1973**, *12*, 232.

(5) Baya, M.; Houghton, J.; Daran, J.-C.; Poli, R. *Angew. Chem., Int. Ed.* **2006**, *46*, 429.

10.1021/ic701826v CCC: $40.75
Published on Web 01/04/2008

$MH_3]^x$ (M = Nb or Ta, $x = 0$; M = Zr, $x = 1-$) are valuable entry points to the chemistry of metallocene complexes, we targeted preparation of their isolobal analogues, $M(NR)_2(PMe_3)(H)_2$ (Mo or W), related to Boncella's complex $W(NPh)\{(NSiMe_3)_2C_6H_4\}(PMe_3)(H)_2$.[9] In the course of this work, we encountered an unusual paramagnetic borohydride compound $Mo(NAr)_2(PMe_3)_2(\eta^2\text{-}BH_4)$ (**1**, Ar = 2,6-$C_6H_3{}^iPr_2$), which lacks strongly π-stabilizing ligands such as CO or an alkene. In this paper we describe synthesis, X-ray structure, and EPR spectra of complex **1**. We also report a DFT study of its electronic and molecular structure and make a comparison with the previously reported ethylene compounds $M(NR)_2(PMe_3)_2(\eta^2\text{-}C_2H_4)$ (M = Mo, R = Ar;[10] M = W, R = Mes = 2,4,6-$C_6H_2Me_3$[11]), the W analogue of which has been the subject of a previous computational study.[12]

Results and Discussion

Synthesis and X-ray Structure of $Mo(NAr)_2(PMe_3)_2(\eta^2\text{-}BH_4)$ (1). Compound **1** was prepared by the addition of a solution of the Mo(VI) bis(imido) compound $Mo(NAr)_2Cl_2(DME)$[13] (Ar = 2,6-$C_6H_3{}^iPr_2$) in THF to a mixture of PMe_3 (ca. 6 equiv) and $NaBH_4$ (1.5 equiv). An initial brown color indicated the in situ formation of an adduct of the type[11] $Mo(NAr)_2Cl_2(PMe_3)_2$, and this was replaced by the green color of $Mo(NAr)_2(PMe_3)_2(\eta^2\text{-}BH_4)$ (**1**) after 2 h. Subsequent workup and crystallization from pentane afforded analytically pure **1** as green crystals in 36% overall yield (eq 1). Compound **1** was characterized by X-ray diffraction analysis and EPR and IR spectroscopy. The ^{1}H NMR spectrum of **1** featured broad resonances consistent with a paramagnetic compound. The IR spectrum showed ν(B−H) bands at 2389, 2358, and 2102 cm^{-1}, consistent with the presence of a bidentate borohydride ligand.[3] The EPR spectra in toluene (fluid and frozen) indicated a d^1 Mo(V) species and are discussed below.

While a large number of Mo(IV) and Mo(VI) bis(imido) compounds are known, compound **1** is a very rare example of a monomeric Mo(V) bis(imido) compound, and only one other has been structurally authenticated (see below).[14] Bis-

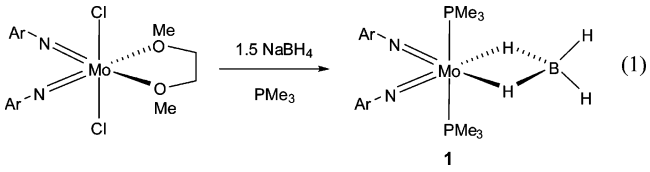

(1)

(imido) Mo(V) compounds are usually dimeric with Mo−Mo bonds.[15−18] Additionally, although transition metal borohydride compounds have been extensively studied,[3,4,19−25] few structurally characterized molybdenum (or Group 6 in general) derivatives are known,[26−29] these all being diamagnetic with formally Mo(0)[26,28,29] or Mo(II) centers.[27] In general, most borohydride complexes complexes conform to the 18 valence electron rule, in particular those with one BH_4 ligand.[24] Paramagnetic borohydride compounds are rather uncommon,[4,19] Finally, we note that imido transition metal borohydrides themselves are unusual[15,16,30,31] and only one example has been structurally authenticated, namely $Ti(NAr)\{ArNC(Me)CHC(Me)CH^tBu\}(\eta^3\text{-}BH_4)$.[32]

The solid-state structure of **1** as determined by X-ray diffraction at 150 K is presented in Figure 1. Selected distances and angles are listed in Table 1 along with those of a DFT computed model $Mo(NAr')_2(PMe_3)_2(\eta^2\text{-}BH_4)$ (**I**, Ar′ = 2,6-$C_6H_3Me_2$) which will be discussed later. All non-hydrogen atoms of **1** were readily located and refined anisotropically. The H atoms of the BH_4 were located from a Fourier difference synthesis and could be positionally refined subject to soft similarity restraints on the B−H distances and with a common isotropic displacement parameter for the H atoms.

(6) (a) Dubberley, S. R.; Ignatov, S. K.; Rees, N. H.; Razuvaev, A. G.; Mountford, P.; Nikonov, G. I. *J. Am. Chem. Soc.* **2003**, *125*, 644. (b) Nikonov, G. I.; Mountford, P.; Dubberley, S. R. *Inorg. Chem.* **2003**, *42*, 58. (c) Nikonov, G. I.; Mountford, P.; Ignatov, S. K.; Green, J. C.; Cooke, P. A.; Leech, M. A.; Kuzmina, L. G.; Razuvaev, A. G.; Rees, N. H.; Blake, A. J.; Howard, J. A. K.; Lemenovskii, D. A. *Dalton Trans.* **2001**, 2903. (d) Ignatov, S. K.; Rees, N. H.; Dubberley, S. R.; Razuvaev, A. G.; Mountford, P.; Nikonov, G. I. *Chem. Commun.* **2004**, 952.

(7) (a) Britovsek, G. J. P.; Gibson, V. C.; Wass, D. F. *Angew. Chem., Int. Ed.* **1999**, *38*, 428. (b) Gibson, V. C.; Spitzmesser, S. K. *Chem. Rev.* **2003**, *103*, 283. (c) Bolton, P. D.; Mountford, P. *Adv. Synth. Catal.* **2005**, *347*, 355.

(8) Ma, K.; Piers, W. E.; Gao, Y.; Parvez, M. *J. Am. Chem. Soc.* **2004**, *126*, 5668.

(9) Boncella, J. M.; Wang, S. Y. S.; Vanderlende, D. D. *J. Electroanal. Chem.* **1999**, *591*, 8.

(10) Dyer, P. W.; Gibson, V. C.; Clegg, W. *J. Chem. Soc., Dalton Trans.* **1995**, 3313.

(11) Radius, U.; Sundermeyer, J.; Pritzkow, H. *Chem. Ber.* **1994**, *127*, 1827.

(12) Radius, U.; Hoffmann, R. *Chem. Ber.* **1996**, *129*, 1345.

(13) Fox, H. H.; Yap, K. B.; Robbins, J.; Cai, S.; Schrock, R. R. *Inorg. Chem.* **1992**, *31*, 2287.

(14) Brandts, J. A. M.; van Leur, M.; Gossage, R. A.; Boersma, J.; Spek, A. L.; van Koten, G. *Organometallics* **1999**, *18*, 2633.

(15) Eikey, R. A.; Abu-Omar, M. M. *Coord. Chem. Rev.* **2003**, *243*, 83.

(16) Wigley, D. E. *Prog. Inorg. Chem.* **1994**, *42*, 239.

(17) Fletcher, D. A.; McMeeking, R. F.; Parkin, D. *J. Chem. Inf. Comput. Sci.* **1996**, *36*, 746 (The United Kingdom Chemical Database Service).

(18) Allen, F. H.; Kennard, O. *Chem. Des. Autom. News* **1993**, *8*, 1, 31.

(19) (a) Marks, T. J.; Kennelly, W. J.; Kolb, J. R.; Shimp, L. A. *Inorg. Chem.* **1972**, *11*, 2540. (b) Desrochers, P. J.; LeLievre, S., Johnson, R. J.; Lamb, B. T.; Phelps, A. L.; Cordes, A. W.; Gu. W.; Cramer, S. P. *Inorg. Chem.* **2003**, *42*, 7945. (c) Mehn, M. P.; Brown, S. D.; Paine, T. K.; Brennessel, W. W.; Cramer, C. J.; Peters, J. C.; Que, L. *Dalton Trans.* **2006**, 1347.

(20) Johnson, P. L.; Cohen, S. A.; Marks, T. J.; Williams, J. M. *J. Am. Chem. Soc.* **1978**, *100*, 2709.

(21) Bell, R. A.; Cohen, S. A.; Doherty, N. M.; Threlkel, R. S.; Bercaw, J. E. *Organometallics* **1986**, *5*, 972.

(22) Green, M. L. H.; Wong, L. L. *J. Chem. Soc., Dalton Trans.* **1989**, 2133.

(23) Lledos, A.; Duran, M.; Jean, Y.; Volatron, F. *Inorg. Chem.* **1991**, *30*, 4440.

(24) Xu, Z.; Lin, Z. *Coord. Chem. Rev.* **1996**, *156*, 139.

(25) Conway, S. L. J.; Doerrer, L. H.; Green, M. L. H.; Leech, M. A. *Organometallics* **2000**, *19*, 630.

(26) Kirtley, S. W.; Andrews, M. A.; Bau, R.; Grynkewich, G. W.; Marks, T. J.; Tipton, D. L.; Whittlesey, B. R. *J. Am. Chem. Soc.* **1977**, *99*, 7154.

(27) Atwood, J. L.; Hunter, W. E.; Carmona-Guzman, E.; Wilkinson, G. *J. Chem. Soc., Dalton Trans.* **1980**, 467.

(28) Tamm, M.; Dressel, B.; Lugger, T.; Frohlich, R.; Grimme, S. *Eur. J. Inorg. Chem.* **2003**, 1088.

(29) Tamm, M.; Dressel, B.; Bannenberg, T.; Grunenberg, J.; Herdtweck, E. *Z. Natuforsch.* **2006**, *61*, 896.

(30) Duncan, A. P.; Bergman, R. G. *Chem. Rec.* **2002**, *2*, 431.

(31) Hazari, N.; Mountford, P. *Acc. Chem. Res.* **2005**, *38*, 839.

(32) Basuli, F.; Bailey, B. C.; Watson, L. A.; Tomaszewski, J.; Huffman, J. C.; Mindiola, D. J. *Organometallics* **2005**, *24*, 1886.

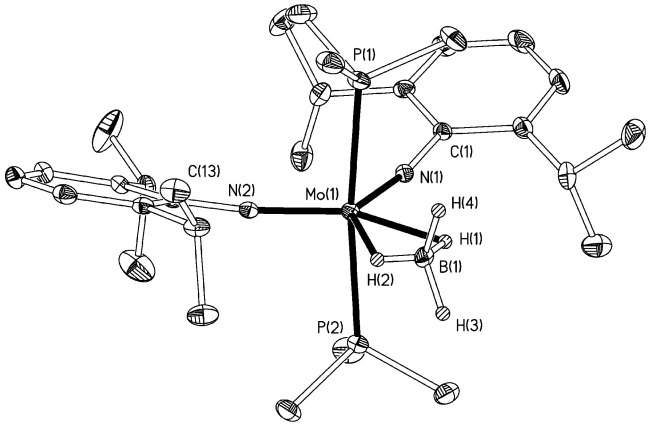

Figure 1. Displacement ellipsoid (20% probability) of Mo(NAr)$_2$(PMe$_3$)$_2$-(η^2-BH$_4$) (**1**). C-bound H atoms are omitted. Other H atoms are drawn as spheres of an arbitrary radius.

Table 1. Selected Experimental Bond Distances (Å) and Angles (deg) for Mo(NAr)$_2$(PMe$_3$)$_2$(η^2-BH$_4$) (**1**) and Those Computed by DFT for the Corresponding Model Mo(NAr′)$_2$(PMe$_3$)$_2$(η^2-BH$_4$) (**I**)

param	**1** (X-ray)	**I** (DFT)
Mo(1)−N(1)	1.822(2)	1.83
Mo(1)−N(2)	1.808(2)	1.81
Mo(1)−P(1)	2.5144(8)	2.47
Mo(1)−P(2)	2.5323(8)	2.47
Mo(1)−H(1)	2.01(1)	1.98
Mo(1)−H(2)	2.00(1)	1.99
Mo(1)···B(1)	2.461(3)	2.40
B(1)−H(1)	1.05(4)	1.26
B(1)−H(2)	0.83(4)	1.26
B(1)−H(3)	1.04(3)	1.22
B(1)−H(4)	1.17(3)	1.22
N(1)−Mo(1)−N(2)	127.59(10)	124
P(1)−Mo(1)−P(2)	173.42(3)	173
N(1)−Mo(1)−B(1)	116.87(11)	117
N(2)−Mo(1)−B(1)	115.03(11)	117
P(1) −Mo(1)−B(1)	86.88(9)	89
P(2) −Mo(1)−B(1)	88.21(9)	85
Mo(1)−N(1)−C(1)	168.5(2)	169
Mo(1)−N(2)−C(13)	172.5(2)	173
H(1)−Mo(1)−H(2)	42.0(15)	63
H(1)−B(1)−H(2)	99.0(17)	111
Ar···Ar[a]	36	33

[a] Angle between the phenyl ring planes

Molecules of **1** contain six-coordinate Mo(V) centers with *cis*-arylimido ligands and *trans*-PMe$_3$ ligands. The atoms of the Mo(μ-H)$_2$B unit are effectively coplanar with the MoN$_2$ moiety. The terminal H atoms (H(3), H(4)) of the borohydride lie above and below this plane with dihedral angles P(1)−Mo(1)···B(1)−H(4) and P(2)−Mo(1)···B(1)−H(3) of 3 and 1°, respectively. The bidentate coordination mode of the BH$_4$ ligand is consistent with the solid-state IR spectrum, and its orientation with regard to the Mo(NAr)$_2$(PMe$_3$)$_2$ fragment is reproduced in the DFT calculations discussed below. The Mo−N−C$_{ipso}$ linkages (168.5(2) and 172.5(2)°) are approximately linear, suggesting that each ArN^{2-} ligand may in principle act as a 6 electron donor[33] to the metal. The electronic structure and bonding in **1** is discussed below.

As mentioned, only one bis(imido) molybdenum(V) compound has been structurally authenticated recently, namely the "ate" complex Mo(NAr)$_2$\{μ,$\kappa_{C,N}^2$-2-C$_6$H$_4$CH$_2$-NMe$_2$\}$_2$Li, which has an approximately tetrahedral Mo(V) center.[14] The Mo−NAr distances in this compound (average 1.771 Å) are somewhat shorter than those in **1** (average 1.815 Å), probably reflecting the higher coordination number of the latter. The ArN−Mo−NAr angle of 121.8 ° (average for two crystallographically independent molecules) is also somewhat less than that in **1** (127.59(10)°). Two structurally characterized bis(arylimido) molybdenum(IV) complexes have been reported previously: Mo(NAr)$_2$(PMe$_3$)$_2$ (average Mo−NAr 1.805 Å, average ArN−Mo−NAr 137°)[34] and Mo-(NAr)$_2$(PMe$_3$)$_2$(η^2-C$_2$H$_4$) (average Mo−NAr 1.828 Å, ArN−Mo−NAr 143.1(2)°).[10] A more comprehensive comparison can be made with a series of molybdenum(VI) five-coordinate bis(arylimido) compounds Mo(NAr)$_2$(L)$_3$ (17 examples: average Mo−NAr 1.75 ± 0.02 Å, average ArN−Mo−NAr 109 ± 7°) and six-coordinate bis(arylimido) compounds Mo(NR)$_2$Cl$_2$L$_2$ (R = 2,6-disubstituted phenyl, 14 examples: average Mo−NAr 1.75 ± 0.03 Å, average ArN−Mo−NAr 104 ± 3°) in general.[17,18] The Mo−NAr distances in **1** are significantly longer than those in either the five- or six-coordinate Mo(VI) compounds, consistent with the higher formal oxidation state of the latter set but rather similar to those of the two Mo(IV) examples. The ArN−Mo−NAr angle of 127.59(10)° in **1** lies between the values for the Mo(IV) and Mo(VI) systems, and this is in accord with theoretical expectations.[12]

Interestingly, the Mo(1)···B(1) distance in **1** (2.461(3) Å) lies at the long end of the limited number of previously characterized molybdenum borohydride compounds, even though its formal oxidation state is significantly higher than in the previous examples: [Mo^0(CO)$_4$(η^2-BH$_4$)]$^-$ (Mo···B = 2.41(2) Å);[26] *trans*-Mo^{II}(PMe$_3$)$_4$(H)(η^2-BH$_4$) (Mo···B = 2.468(12) Å);[27] Mo^0(η^7,η^1-C$_7$H$_6$-2-C$_6$H$_4$P^{i}Pr$_2$)-(η^2-BH$_4$) (Mo···B = 2.358 Å[35]);[28] Mo^0(η-C$_7$H$_7$)(PCy$_3$)(η^2-BH$_4$) (Mo···B = 2.379 Å[36]).[29]

EPR Spectra. The EPR spectra of **1** as frozen and fluid toluene solutions are shown in Figure 2 along with their simulations. The spectra are characteristic of an $S = 1/2$ species, consistent with the formulation of Mo(NAr)$_2$(PMe$_3$)$_2$-(η^2-BH$_4$) (**1**) as a Mo(V), d^1 compound. The fluid solution spectrum shows a central 1:2:1 triplet hyperfine multiplet, centered on $g_{iso} = 1.969$. This is either due to interaction of the unpaired electron (upe) with two equivalent ^{31}P nuclei ($I = 1/2$, 100%) or with the two coordinated ^{1}H's ($I = 1/2$, 100%) of BH$_4^-$. However, the former possibility may be the more likely since ^{31}P gives inherently larger hyperfine couplings than ^{1}H. Further transitions are observed in the wings of the spectrum, and these are satellites due to hyperfine coupling of the upe with ^{95,97}Mo (nuclear spin $I = {}^5/_2$, sum to 25% natural abundance). The individual contributions from the two isotopes were not resolved. The hyperfine coupling constants to ^{95,97}Mo and P are coincidently similar, and simulation gives a_{iso}(P) = 27 × 10^{-4} and A_{iso}-(Mo) = 25 × 10^{-4} cm^{-1}. The solution g_{iso} and A_{iso}(Mo)

(33) Using the anionic donor formalism.

(34) Dyer, P. W.; Gibson, V. C.; Howard, J. A. K.; Wilson, C. *J. Organomet. Chem.* **1993**, *462*, C15.
(35) Esd not reported.
(36) Esd not reported.

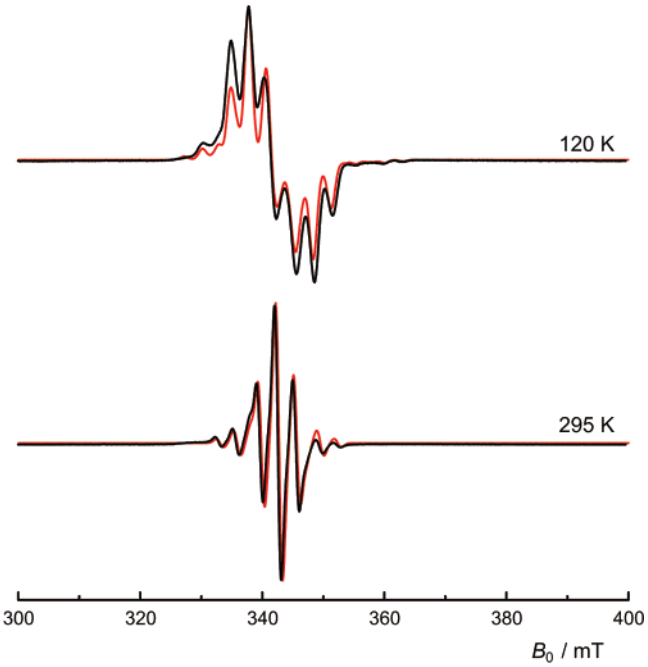

Figure 2. EPR spectra (black line) of the frozen solution (top) and fluid solution (bottom) of $Mo(NAr)_2(PMe_3)_2(\eta^2\text{-}BH_4)$ (**1**) in toluene and their simulation (red line).

values for **1** are comparable to those reported for $Mo(NAr)_2\{\mu,\kappa_{C,N}{}^2\text{-}2\text{-}C_6H_4CH_2NMe_2\}_2Li$.[14]

The frozen solution spectrum show an overlapping rhombic pattern of *g*-values (rhombic symmetry), each of which is split into 1:2:1 triplet by the interaction of the upe with two equivalent ^{31}P (probably) or ^1H atoms. Again, additional features due to the Mo satellites are observed in the wings of the spectrum. Simulation gives the anisotropic EPR parameters $g_1 = 1.998$, $g_2 = 1.977$, and $g_3 = 1.937$ with $a_1(P) = a_2(P) = a_3(P) = 27 \times 10^{-4}$ cm^{-1} and $A_1(Mo) = 28.0 \times 10^{-4}$, $A_2(Mo) = 4 \times 10^{-4}$, and $A_3(Mo) = 27 \times 10^{-4}$ cm^{-1}.[37] The ^{31}P (or ^1H) hyperfine coupling is isotropic within the resolution of the experiment, while that to Mo is considerably anisotropic. The isotropic and anisotropic *g*-values are all less than 2.0023 (free electron value), consistent with **1** being Mo(V), d^1. The rhombic EPR symmetry [in terms of *g* and *A*(Mo)] is consistent with the approximate C_{2v} symmetry of the $\{MoP_2N_2B\}$ coordination sphere found in the solid state.

DFT Studies: Electronic Structure. Compound **1** raises a number of interesting questions concerning its geometry and electronic structure. The effectively linear Ar−N−Mo linkages suggest that each ArN^{2-} may act as a 6 electron donor (1 σ + 2 π interaction) to the d^1 metal.[38] Likewise, the bidentate BH_4^- is able to act as a formal 4-electron donor through a σ and π type interaction.[24] Hence, the Mo center in compound **1** could (after taking into account σ donation from the axial PMe_3 ligands) in principle achieve a maximum valence electron count of 21.

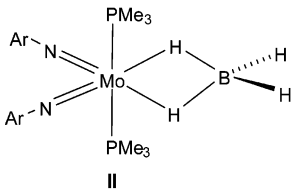

II

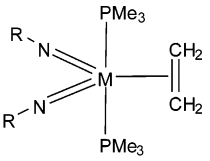

M = Mo, R = Ar (**III**)
M = W, R = Mes (**VI**)

A second interesting question concerns the pseudooctahedral geometry found experimentally for **1** in which the H atoms of the $Mo(\mu\text{-}H)_2B$ unit are coincident with the N_2Mo plane (Figure 1). Although this geometry is analogous to that found in numerous 6-coordinate d^0 Mo(VI) bis(imido) compounds of the type $Mo(NR)_2X_2(L)_2$,[15,16,38] it is not necessarily clear why **1** would not adopt an alternative geometry (**II**) in which the $Mo(\mu\text{-}H)_2B$ unit is rotated by 90° to be coincident with the P−Mo−P axis and avoid having B−H bonds opposite the strongly trans-labilizing ArN ligands. Such a geometry is found in the solid state for the d^2 Mo(IV) and W(IV) ethylene complexes $M(NR)_2(PMe_3)_2(\eta^2\text{-}C_2H_4)$ (M = Mo, R = Ar (**III**);[10] M = W, R = Mes (**IV**)[11]). These two aspects have been addressed using symmetry analyses and DFT calculations as discussed below.

In the DFT calculations the isopropyl groups of **1** were replaced by methyl groups in the model complex $Mo(NAr')_2(PMe_3)_2(\eta^2\text{-}BH_4)$ (**I**). The geometry optimized structure is shown in Figure 3, and selected geometric parameters are compared with the X-ray crystal structure in Table 1. A doublet ground state was found to be the lowest in energy. Overall, the calculation accurately reproduces the experimental structure of **1** with a slight underestimation of the Mo−P and Mo···B distances, which may arise from decreased steric repulsion of the PMe_3 ligands due to the approximation of modeling the isopropyl substituents by the smaller methyl groups. The calculated Mo−N bond distances are in excellent agreement with the experimental ones. Interestingly, the angle between the two of the phenyl rings of the aromatic imido ligands observed in the crystal structure (36°) is accurately reproduced in the calculations (33°), despite the replacement of the isopropyl groups with methyl groups. This suggests that the driving force for twisting is electronic in nature with negligible contribution from steric effects. The imido groups are not cylindrically symmetric, and the out of plane N 2pπ orbitals are higher in energy than the in-plane ones.[39] The twist helps lessen the competition of these N pπ orbital for donation into the same Mo d orbital. If one excludes all hydrogen atoms and the carbon atoms of the two methyl groups of the isopropyl substituents, the calculated root-mean-square deviation between the crystal structure and the optimized structure is only 0.09996. This indicates that the calculations provide an excellent representation model for complex **1**, which gives confidence in further analysis of the bonding within the system.

Examination of the unrestricted (α- and β-spin) molecular orbitals (MOs) reveals a number of interesting features. The

(37) Only the Mo hyperfine couplings to g_1 and g_3 are observable; hence, these parameters can be determined by simulation while A_2(Mo) is determined from the relationship $A_{iso} = (A_1 + A_2 + A_3)/3$.

(38) Nugent, W. A.; Mayer, J. M. *Metal-Ligand Multiple Bonds*; Wiley-Interscience: New York, 1988.

(39) Dunn, S. C.; Hazari, N.; Jones, N. M.; Moody, A. G.; Blake, A. J.; Cowley, A. R.; Green, J. C.; Mountford, P. *Chem.—Eur. J.* **2005**, *11*, 2111.

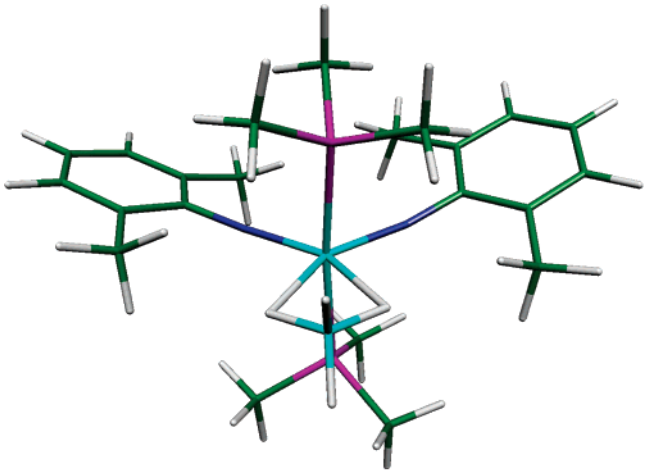

Figure 3. DFT-optimized geometry of the model complex Mo(NAr′)$_2$(PMe$_3$)$_2$(η^2-BH$_4$) (**I**).

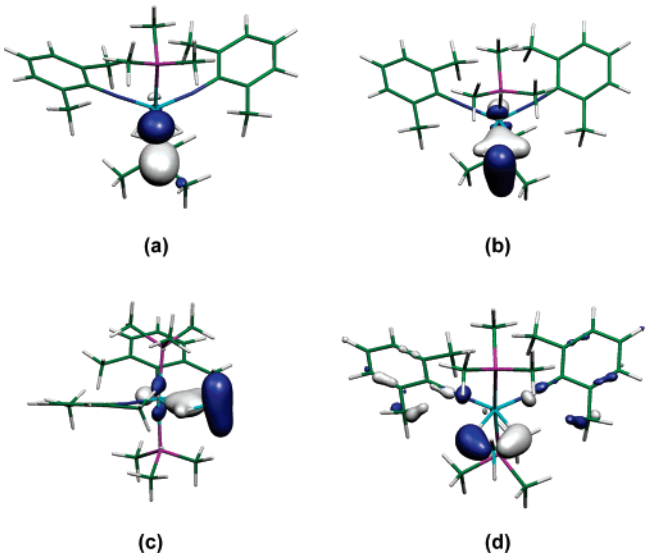

Figure 4. Molecular orbital isosurfaces of the α-spin orbitals of **I** involving the borohydride ligand: (a) HOMO-8; (b) HOMO-9; (c) HOMO-9 side view; (d) HOMO-10.

β-spin orbitals closely resemble the α-spin orbitals. Using the ionic method of counting valence electrons, the Mo atom donates two electrons to each of the imido ligands and one electron to the borohydride ligand formally producing a Mo(V) ion, with a d^1 electron configuration. The imido ligands are then counted as 6 electron donors, two electrons are donated from each of the trimethylphosphine ligands, one electron resides on the Mo(V) ion, and, depending on the bonding situation, the BH_4^- anionic ligand may act as either a 2 or 4 electron donor.[24] The MOs derived from the BH_4^- t_2 set (αHOMO-8, αHOMO-9, and αHOMO-10) (Figure 4) show a significant σ interaction with the Mo, but an absence of π interaction that might be expected through the bridging H atoms, which suggests that the BH_4 group is effectively acting as a 2 electron donor in complex **1**. A fragment calculation indicates that σ donation from BH_4^- is 0.36 electrons while π donation is 0.22 electrons. In terms of competitive π loading, the BH_4^- group loses out to the more effective π-donor imido ligands.[40] This appears to be consistent with the long Mo(1)···B(1) distance noted above for the experimental and computed structure of **1** and **I**, respectively.

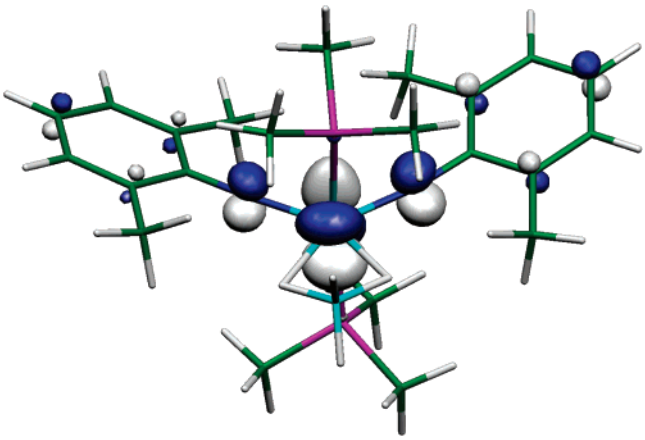

Figure 5. Molecular orbital electron density isosurface of the occupied αHOMO. This orbital represents the singly occupied molecular orbital (SOMO) of complex **1** probed by the EPR experiment.

The unpaired electron resides in the Mo−N π* antibonding αHOMO (Figure 5) for which the lowest unoccupied β-spin orbital (βLUMO) is the spatial counterpart. Therefore, we conclude that **1** is best classified as a 19 valence electron Mo(V) complex. Thus, **1** proves an exception to the rule formulated by Xu and Lin that most of the transition-metal tetrahydroborato complexes conform to the 18 electron rule, especially those complexes with only one BH_4 ligand.[24]

In the d^2 M(IV) complexes, M(NR)$_2$(PMe$_3$)$_2$(η^2-C$_2$H$_4$) (M = Mo, R = Ar (**III**);[10] M = W, R = Mes = 2,4,6-C$_6$H$_2$Me$_3$ (**IV**)[11]), the two d electrons reside in an analogous orbital which promotes back-donation into the coordinated olefin[12] and, hence, the observed alignment of the C═C vector perpendicular to the N−M−N plane. In **1**, the BH_4 ligand (which is not a π acceptor) orients such that the coordinating bridging μ-H atoms lie in the nodal plane of this orbital and thus avoid an antibonding interaction with the unpaired electron. Furthermore, DFT calculations revealed that the pseudooctahedral geometry observed for model complex **I** was 40 kJ mol^{-1} more stable in comparison to the axial orientation of the Mo(μ-H)$_2$B unit shown above in **II** (parallel to the P−Mo−P axis). In addition, the Mo···B distance increased from 2.47 Å in **I** to 2.84 Å in the geometry-optimized structure **II**, with a corresponding change to an η^1 BH_4 coordination mode. No significant differences were observed between the molecular orbital structures of **I** and **II**, which indicates that the BH_4^- ligand is relatively weakly bound and that its bonding to Mo is mostly electrostatic in nature in **1**. There was in addition a lengthening of the bonds to imido ligands by 0.01 Å and the angle between the planes of the phenyl rings reduced to 7°.

DFT Studies: EPR Calculations. The unpaired spin density mirrors the spatial distribution of the αHOMO orbital, and although primarily located on the Mo ion, significant spin-density delocalization onto the two N atoms occurs with rather minor delocalization onto the P atoms (Figure 5 and Table 2).

(40) Lin, Z.; Hall, M. B. *Coord. Chem. Rev.* **1993**, *123*, 149.

Table 2. Calculated Atomic Spin Densities for $Mo(NAr)_2(PMe_3)_2(\eta^2\text{-}BH_4)$ (**I**) from Gaussian 03 (Mulliken and NPA) and ADF DFT Calculations[a]

	spin density		
	Gaussian 03		
	Mulliken	NPA	ADF (Mulliken)
Mo(1)	0.591	0.449	0.533
P(1)	−0.019	0.019	0.021
P(2)	0.010	0.018	0.015
N(1)	0.136	0.165	0.097
N(2)	0.073	0.104	0.061
C(1)	−0.073	−0.042	−0.013
C(13)	−0.040	−0.029	−0.010
B(1)	−0.027	−0.006	−0.008
$H_{bridge}(1)$	−0.004	−0.001	−0.003
$H_{bridge}(2)$	−0.005	−0.002	−0.003
$H_{terminal}(4)$	0.011	0.008	0.011
$H_{terminal}(3)$	0.012	0.010	0.013

[a] Atom labels correspond to those for the crystal structure of **1** (Figure 1).

Table 3. Comparison of Experimental EPR Parameters for $Mo(NAr)_2(PMe_3)_2(\eta^2\text{-}BH_4)$ (**1**) with Those Calculated for $Mo(NAr')_2(PMe_3)_2(\eta^2\text{-}BH_4)$ (**I**) for Various Basis Sets[a]

		I		
param	**1** (expt)	TZP	TZ2P	QZ4P
$\mathbf{g_{iso}}$	**1.969**	**1.9846**	**1.9847**	**1.9845**
$\boldsymbol{A_{iso}}$**(Mo(1))**	**25**	**11.7597**	**12.0644**	**12.4714**
A_{iso}(P(1))	*b*	29.1961	27.2946	27.2118
A_{iso}(P(2))	*b*	34.8895	32.9739	33.5774
$\boldsymbol{A_{iso}}$**(P)**$_{av}$	**27**	**32.0428**	**30.1343**	**30.3946**
A_{iso}(N(1))	*b*	−0.0241	−0.0574	−0.0730
A_{iso}(N(2))	*b*	−0.3978	−0.4191	−0.4181
A_{iso}(N) avg	*b*	−0.2110	−0.2383	−0.2456
$A_{iso}(H_{bridge}(1))$	*b*	−1.6916	−1.7216	−1.2328
$A_{iso}(H_{bridge}(2))$	*b*	−1.9231	−1.9540	−0.0393
$A_{iso}(H_{bridge})_{av}$	*b*	−1.8073	−1.8378	−0.6360

[a] The g_{iso} values are dimensionless, and the hyperfine coupling constants (hfc) are in units of 1.0×10^{-4} cm^{-1}. [b] Not determined.

The location of the spin density suggests that the unpaired electron should couple strongly to the molybdenum atom and also possibly to the two nitrogen atoms of the imido ligands. However, the experimental spectrum indicates that the unpaired electron couples strongly to two equivalent phosphorus atoms in addition to the Mo nucleus. To elucidate this coupling pattern, calculations of the hyperfine coupling (hfc) constants were performed using the DFT-optimized geometry of **I**. The results are summarized in Table 3.

The EPR calculations using spin−orbit relativistic effects are remarkably consistent even with increasing basis set size. If one moves from the all electron TZP to the QZ4P basis set, the calculated value of g_{iso} changes only in the fourth decimal place and all calculations overestimated g_{iso} with respect to the experimental value by around 0.016. The calculated isotropic hfc constant for Mo is relatively low (ca. 12×10^{-4} cm^{-1}) and approximately half of the value observed experimentally. Such errors are not uncommon in the calculation of transition metal hyperfine coupling.[41,42] The average isotropic hfc constant for the two phosphorus nuclei is calculated to be between 30.1×10^{-4} and 32.0×10^{-4} cm^{-1}, which is in very good agreement with the experimental value of 27×10^{-4} cm^{-1}. Using the TZ2P basis set gives the best quantitative estimate of A_{iso}(P), and interestingly, the calculated hfc constants indicate that the two phosphorus nuclei are inequivalent in the gas-phase optimized geometry, even though the Mo−P distances are approximately equal (calculated difference is 0.003 Å). The N A_{iso} values are also rather different but less so in terms of absolute magnitude. Given the resolution and time scale of the EPR experiment, the hfc constants to the two phosphorus nuclei were found to be equivalent in solution phase.

Despite the high spin density values on the two nitrogen atoms of the imido ligands, the EPR calculations indicate that the nitrogen nuclei and, indeed, the two bridging hydrogen atoms from the borohydride ligand couple only weakly to the unpaired electron. Therefore, the EPR calculations support the assignment that the splitting pattern observed is due to the unpaired electron coupling to the Mo and P nuclei. The reason that coupling to the nitrogen atoms is not observed is due to the nature of the αHOMO. Figure 5 shows that this orbital is π^* antibonding with respect to the nitrogen and molybdenum atoms. The d_{yz}, d_{xz}, and $d_{x^2-y^2}$ orbitals on the molybdenum contribute 20.1, 13.0, and 5.2% of the total MO character with the next major contributions from the nitrogen p_z orbitals (8.5 and 8.1%). Minor contributions are also observed for the conjugated p_z orbitals of the *ortho*- and *para*-ring carbon atoms. The spin density is localized in an orbital which has negligible s-orbital character. Therefore, the coupling of unpaired electron density to the nitrogen nuclei can only occur via spin polarization which is much weaker than s-orbital (Fermi contact) coupling. The P atoms form a strong σ-interaction with the Mo ion, with high s-orbital contributions. This increases the coupling between the unpaired electron and the nuclei, which consequently leads to the splitting patterns observed in the EPR experiments.

As mentioned, the $Mo-BH_4$ bonding has a large electrostatic component, and in the limiting case, **1** could be viewed as a tight ion pair $[Mo(NAr)_2(PMe_3)_2]^+[BH_4]^-$ containing a Mo(V) d^1 17 valence electron cation. This system would still be EPR active with $S = 1/2$. The crystal structure of the neutral Mo(IV) d^2 species, $[Mo(NAr)_2(PMe_3)_2]$, has been reported and shows a tetrahedral disposition of the four ligands.[34] The DFT geometry (Figure 6) of the model cation $[Mo(NAr')_2(PMe_3)_2]^+$ (**V**) is very similar that of **I** and the Mo center has a tetrahedral coordination environment. EPR calculations were also performed on this 17 valence electron molybdenum cation, but the values obtained for the **g** tensors and the hyperfine coupling constants were not sufficiently different from those calculated for **I** to provide evidence either way for this being a fair representation of the solution structure. Experimentally, it is unlikely that the strongly coordinating and polarizable BH_4^- anion would dissociate from a $[Mo(NAr)_2(PMe_3)_2]^+$ cation in a low dielectric solvent such as toluene.

(41) Morley, G. W.; Herbert, B. J.; Lee, S. M.; Porfyrakis, K.; Dennis, T. J. S.; Nguyen-Manh, D.; Scipioni, R.; van Tol, J.; Horsfield, A. P.; Ardavan, A.; Pettifor, D. G.; Green, J. C.; Briggs, G. A. D. *Nanotechnology* **2005**, *16*, 2469.

(42) Kessler, B.; Bringer, A.; Cramm, S.; Schlebusch, C.; Eberhardt, W.; Suzuki, S.; Achiba, Y.; Esch, F.; Barnaba, M.; Cocco, D. *Phys. Rev. Lett.* **1997**, *79*, 2289.

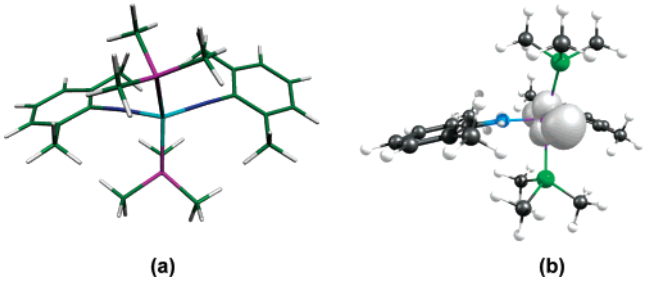

Figure 6. (a) DFT geometry of [Mo(NAr′)$_2$(PMe$_3$)$_2$]$^+$ (**V**) and (b) isosurface of the residual SCF spin density (α minus β spin densities).

Conclusion

Reaction of Mo(NAr)$_2$Cl$_2$(DME) (Ar = 2,6-C$_6$H$_3$^{i}Pr$_2$) with NaBH$_4$ and PMe$_3$ gave the paramagnetic Mo(V) d^1 borohydride complex Mo(NAr)$_2$(PMe$_3$)$_2$(η^2-BH$_4$) (**1**). Unusually, the BH$_4^-$ ligand acts mainly as a σ donor to the Mo(V) center to form a formally 19 valence electron species. The bonding between the BH$_4^-$ ligand and the Mo(V) cationic center has a significant electrostatic component. The assignment of the experimental EPR spectrum was consistent with the DFT calculations. Although the spin density was calculated to be significantly higher on N than P atoms, coupling to ^{31}P predominated in the EPR spectrum. These findings underline the danger of making deductions as to relative spin density on atoms directly from the magnitudes of the observed hyperfine splittings.

Experimental Section

General Methods and Instrumentation. All air- and moisture-sensitive operations were carried out using standard Schlenk-line (Ar) and drybox (N$_2$) techniques. Protio and deutero solvents were purified, dried, and distilled using conventional techniques. The ^{1}H NMR spectrum was recorded on a Varian Mercury-*vx* (^{1}H, 300 MHz) spectrometer. The IR spectrum was recorded on a Perkin-Elmer Paragon 1000 FT-IR spectrometer as a Nujol mull between NaCl windows, and data are quoted in wavenumbers (cm^{-1}). The X-band (9.450 GHz) EPR spectra were recorded at 120 and 295 K using a Bruker EMX spectrometer and were analyzed using the Bruker programs WINEPR and XSophie. Elemental analyses were carried out by the analytical laboratory of the Inorganic Chemistry Laboratory, University of Oxford.

Starting Materials. Mo(NAr)$_2$Cl$_2$(DME)[13] and PMe$_3$[43] were prepared according to the literature methods. NaBH$_4$ was obtained from Sigma-Aldrich and used without further purification.

Synthesis of Mo(NAr)$_2$(PMe$_3$)$_2$(η^2-BH$_4$). A solution of Mo(NAr)$_2$Cl$_2$(DME) (0.364 g, 0.60 mmol) in THF (15 mL) was added to a mixture of NaBH$_4$ (0.35 g, 0.925 mmol) and PMe$_3$ (0.40 mL, 3.86 mmol). Upon addition of the reagents, the color turned dark brown due to the in situ formation of Mo(NAr)$_2$Cl$_2$(PMe$_3$)$_2$. The mixture was stirred for 2 h, during which time it became dark green. The volatiles were removed under reduced pressure, the residue was extracted into diethyl ether (20 mL), and the extract was filtered. The dark solid produced after evaporation of the volatiles is a mixture of **1** and an impurity, Mo(NAr)Cl$_2$(PMe$_3$)$_3$, according ^{1}H NMR spectroscopy. Recrystallization from pentane (30 mL) at −30 °C afforded **1** as well-formed dark green crystals, which were collected by filtration, washed with the minimum amount of cold pentane, and dried in vacuo. Yield: 0.084 g. A second crop (0.050 g) was obtained in a similar fashion from the concentrated mother liquors. Combined yield: 0.134 g (36%). IR (selected bands): 2389, 2358, and 2102 cm^{-1}. ^{1}H NMR (C$_6$D$_6$): two very broad, featureless resonances at ca. 4.6 and 3.7 ppm due to the paramagnetic nature of the compound. Anal. Found (calcd for C$_{30}$H$_{56}$BMoN$_2$P$_2$): C, 58.24 (58.73); H, 9.07 (9.20); N, 4.38 (4.57).

Table 4. X-ray Data Collection and Processing Parameters for Mo(NAr)$_2$(PMe$_3$)$_2$(η^2-BH$_4$) (**1**)

empirical formula	C30H$_{56}$BMoN$_2$P$_2$	β/deg	93.3190(14)
fw	613.49	γ/deg	107.7986(11)
temp/K	150	V/Å^3	1737.88(9)
wavelength/Å	0.710 73	Z	2
space group	$P\bar{1}$	d(calcd)/Mg·m^{-3}	1.172
a/Å	11.2581(3)	abs coeff/mm^{-1}	0.489
b/Å	12.8096(4)	R_1	0.0452 [$I > 2\sigma(I)$]
c/Å	13.0998(4)	$wR2$	0.1077 (all data)
α/deg	102.8021(14)		

EPR Spectra. Mo(NAr)$_2$(PMe$_3$)$_2$(η^2-BH$_4$) (**1**) was dissolved in toluene in a glovebox. Immediately after preparation, samples were frozen in liquid N$_2$. The X-band EPR spectra of **1** were recorded at 120 and 295 K. Frozen solution spectra were measured first, and then the samples were allowed to thaw (still under an inert atmosphere) and fluid solution spectra measured at room temperature.

Crystal Structure Determination. Data collection and processing parameters are given in Table 4. A crystal of **1** was mounted on a glass fiber using perfluoropolyether oil and cooled rapidly in a stream of cold N$_2$ using an Oxford Cryosystems CRYOSTREAM unit. Diffraction data were measured using an Enraf-Nonius KappaCCD diffractometer. Intensity data were processed using the DENZO-SMN package.[44] The structures were solved using SIR92,[45] which located all non-hydrogen atoms. Subsequent full-matrix least-squares refinement was carried out using the CRYSTALS program suite.[46] Coordinates and anisotropic thermal parameters of all non-hydrogen atoms were refined (see additional comments below). C-bound H atoms were placed geometrically and refined in a riding model. The H atoms of the BH$_4$ group were located in a Fourier difference synthesis and refined isotropically and positionally subject to soft restraints on the B−H and Mo−H bond parameters. An equivalent isotropic displacement parameter was refined for the BH$_4$ H atoms. A Chebychev weighting scheme was applied for the final cycles of refinement.

A full listing of atomic coordinates, bond lengths and angles, and displacement parameters for Mo(NAr)$_2$(PMe$_3$)$_2$(η^2-BH$_4$) (**1**) has been deposited at the Cambridge Crystallographic Data Center. See Notice to Authors, Issue No. 1.

Computational Details. Density functional theory calculations were performed using ADF 2006.01[47] and Gaussian 03, revision D.01, quantum chemical programs.[48] A simplified model, Mo(NAr′)$_2$(PMe$_3$)$_2$(η^2-BH$_4$) (**I**, Ar′ = 2,6-C$_6$H$_3$Me$_2$), was investigated where the four isopropyl groups of **1** were substituted by methyl groups. Geometry optimizations were performed in ADF. The local density approximation (LDA) employed the VWN functional,[49] and gradient corrections were applied post-SCF using the BP86

(43) Wolfsberger, W.; Schmidbauer, H. *Synth. React. Inorg. Met.-Org. Chem.* **1974**, *4*, 149.
(44) Otwinowski, Z.; Minor, W. *Processing of X-ray Diffraction Data Collected in Oscillation Mode*; Academic Press: New York, 1997.
(45) Altomare, A.; Cascarano, G.; Giacovazzo, G.; Guagliardi, A.; Burla, M. C.; Polidori, G.; Camalli, M. *J. Appl. Crystallogr.* **1994**, *27*, 435.
(46) Betteridge, P. W.; Cooper, J. R.; Cooper, R. I.; Prout, K.; Watkin, D. J. *J. Appl. Crystallogr.* **2003**, *36*, 1487.

exchange-correlation functionals.[47,50−52] Scalar relativistic effects were incorporated using the ZORA formalism,[53−55] and a TZP basis set was used with small frozen cores for the heavy atoms (Mo 2p, P 2p, N 1s, C 1s, B 1s). The convergence criteria used for geometry optimizations were: energy = 5.00×10^{-4} au; grad = 5.00×10^{-3} au; rad = 5.00×10^{-3} Å; angle = 0.50°. All calculations performed were unrestricted and used an integration grid of 6.0. Harmonic frequency analysis based on analytical second derivates[56−58] was used to characterize the optimized geometries as local minima on the potential energy surface (PES). For a doublet ground state, the squared spin angular momentum, S^2, should equal 0.75. The value of S^2 obtained from the ADF calculation is 0.7513, which indicates that there is minimal spin contamination. Hyperfine coupling constants[59] and **g**-tensors[60] were calculated in ADF by the implementation of van Lenthe. Geometry-optimized structures were used in single point calculations with all electron basis sets of increasing size, (TZP, TZ2P, and QZ4P) to calculate isotropic hyperfine coupling constants and g_{iso} values.

The bonding was investigated using natural bond orbital (NBO) analysis implemented in Gaussian 03.[61] A single point calculation on the ADF-optimized structure was performed using the B3LYP exchange-correlation functionals.[50,62] The double-ζ basis set, 6-31+G-(d,p), was used for the description of the C, N, P, B, and H atoms.[63−68] The SDD ECP basis set was used for molybdenum.[69,70]

Cartesian coordinates for **I**, **II**, and **V** are given in the Supporting Information.

Acknowledgment. We thank the EPSRC (J.P.H.) and the Royal Society (Project Grant to P.M. and G.I.N) for support and Dr. A. R. Cowley for collecting the X-ray diffraction data. G.I.N. thanks Brock University for additional financial support. We also thank the Oxford Supercomputing Centre.

Supporting Information Available: X-ray crystallographic data in CIF format for the structure determinations of $Mo(NAr)_2(PMe_3)_2(\eta^2\text{-}BH_4)$ (**1**) and Cartesian coordinates of the gas-phase DFT-optimized structures **I**, **II**, and **V**. This material is available free of charge via the Internet at http://pubs.acs.org.

IC701826V

(47) Baerends, E. J.; Autschbach, J.; Bérces, A.; Bickelhaupt, F. M.; Bo, C.; Boeij, P. L. d.; Boerrigter, P. M.; Cavallo, L.; Chong, D. P.; Deng, L.; Dickson, R. M.; Ellis, D. E.; Fan, L.; Fischer, T. H.; Guerra, C. F.; Gisbergen, S. J. A. v.; Groeneveld, J. A.; Gritsenko, O. V.; Grüning, M.; Harris, F. E.; Hoek, P. v. d.; Jacob, C. R.; Jacobsen, H.; Jensen, L.; Kessel, G. v.; Kootstra, F.; Lenthe, E. v.; McCormack, D. A.; Michalak, A.; Neugebauer, J.; Osinga, V. P.; Patchkovskii, S.; Philipsen, P. H. T.; Post, D.; Pye, C. C.; Ravenek, W.; Ros, P.; Schipper, P. R. T.; Schreckenbach, G.; Snijders, J. G.; Solà, M.; Swart, M.; Swerhone, D.; Velde, G. t.; Vernooijs, P.; Versluis, L.; Visscher, L.; Visser, O.; Wang, F.; Wesolowski, T. A.; Wezenbeek, E. v.; Wiesenekker, G.; Wolff, S. K.; Woo, T. K.; Yakovlev, A. L.; Ziegler, T. *SCM*; Theoretical Chemistry, Vrije Universiteit: Amsterdam, 2006 (http://www.scm.com).

(48) Frisch, M. J.; Trucks, G. W.; Schlegel, H. B.; Scuseria, G. E.; Robb, M. A.; Cheeseman, J. R.; Montgomery, J. A., Jr.; Vreven, T.; Kudin, K. N.; Burant, J. C.; Millam, J. M.; Iyengar, S. S.; Tomasi, J.; Barone, V.; Mennucci, B.; Cossi, M.; Scalmani, G.; Rega, N.; Petersson, G. A.; Nakatsuji, H.; Hada, M.; Ehara, M.; Toyota, K.; Fukuda, R.; Hasegawa, J.; Ishida, M.; Nakajima, T.; Honda, Y.; Kitao, O.; Nakai, H.; Klene, M.; Li, X.; Knox, J. E.; Hratchian, H. P.; Cross, J. B.; Bakken, V.; Adamo, C.; Jaramillo, J.; Gomperts, R.; Stratmann, R. E.; Yazyev, O.; Austin, A. J.; Cammi, R.; Pomelli, C.; Ochterski, J. W.; Ayala, P. Y.; Morokuma, K.; Voth, G. A.; Salvador, P.; Dannenberg, J. J.; Zakrzewski, V. G.; Dapprich, S.; Daniels, A. D.; Strain, M. C.; Farkas, O.; Malick, D. K.; Rabuck, A. D.; Raghavachari, K.; Foresman, J. B.; Ortiz, J. V.; Cui, Q.; Baboul, A. G.; Clifford, S.; Cioslowski, J.; Stefanov, B. B.; Liu, G.; Liashenko, A.; Piskorz, P.; Komaromi, I.; Martin, R. L.; Fox, D. J.; Keith, T.; Al-Laham, M. A.; Peng, C. Y.; Nanayakkara, A.; Challacombe, M.; Gill, P. M. W.; Johnson, B.; Chen, W.; Wong, M. W.; Gonzalez, C.; Pople, J. A. *Gaussian 03*, revision C.02; Gaussian, Inc.: Wallingford, CT, 2004.

(49) Vosko, S. H.; Wilk, L.; Nusair, M. *Can. J. Phys.* **1980**, *58*, 1200.

(50) Becke, A. D. *Phys. Rev. A* **1988**, *38*, 3098.

(51) Becke, A. D. *J. Chem. Phys.* **1988**, *88*, 1053.

(52) Perdew, J. P. *Phys. Rev. B* **1986**, *34*, 7406.

(53) van Lenthe, E.; Ehlers, A.; Baerends, E.-J. *J. Chem. Phys.* **1999**, *110*, 8943.

(54) van Lenthe, E.; Baerends, E. J.; Snijders, J. G. *J. Chem. Phys.* **1994**, *101*, 9783.

(55) van Lenthe, E.; Baerends, E. J.; Snijders, J. G. *J. Chem. Phys.* **1993**, *99*, 4597.

(56) Jacobsen, H.; Berces, A.; Swerhone, D. P.; Ziegler, T. *Comput. Phys. Commun.* **1997**, *100*, 263.

(57) Berces, A.; Dickson, R. M.; Fan, L.; Jacobsen, H.; Swerhone, D.; Ziegler, T. *Comput. Phys. Commun.* **1997**, *100*, 247.

(58) Wolff, S. K. *Int. J. Quantum Chem.* **2005**, *104*, 645.

(59) van Lenthe, E.; van der Avoird, A.; Wormer, P. E. S. *J. Chem. Phys.* **1998**, *108*, 4783.

(60) van Lenthe, E.; Wormer, P. E. S.; van der Avoird, A. *J. Chem. Phys.* **1997**, *107*, 2488.

(61) Reed, A. E.; Curtiss, L. A.; Weinhold, F. *Chem. Rev.* **1988**, *88*, 899.

(62) Lee, C.; Yang, W.; Parr, R. G. *Phys. Rev. B* **1988**, *37*, 785.

(63) Hehre, W. J.; Ditchfield, R.; Pople, J. A. *J. Chem. Phys.* **1972**, *56*, 2257.

(64) Hariharan, P. C.; Pople, J. A. *Theor. Chim. Acta* **1973**, *28*, 213.

(65) Hariharan, P. C.; Pople, J. A. *Mol. Phys.* **1974**, *27*, 209.

(66) Francl, M. M.; Pietro, W. J.; Hehre, W. J.; Binkley, J. S.; Gordon, M. S.; DeFrees, D. J.; Pople, J. A. *J. Chem. Phys.* **1982**, *77*, 3654.

(67) Rassolov, V. A.; Pople, J. A.; Ratner, M. A.; Windus, T. L. *J. Chem. Phys.* **1998**, *109*, 1223.

(68) Rassolov, V. A.; Ratner, M. A.; Pople, J. A.; Redfern, P. C.; Curtiss, L. A. *J. Comput. Chem.* **2001**, *22*, 976.

(69) Andrae, D.; Haeussermann, U.; Dolg, M.; Stoll, H.; Preuss, H. *Theor. Chim. Acta* **1991**, *78*, 247.

(70) Andrae, D.; Haussermann, U.; Dolg, M.; Stoll, H.; Preuss, H. *Theor. Chim. Acta* **1990**, *77*, 123.